





Spin dynamics in two ReF_6 -based single-molecule magnets from NMR and ac susceptibility measurements

Oleg M. Vyaselev ^{1,*}, Nataliya D. Kushch ², Eduard B. Yagubskii², Olga V. Maximova ^{3,4} and Alexander N. Vasiliev ^{3,5,6}

¹*Institute of Solid State Physics, Russian Academy of Sciences, Chernogolovka, Moscow Region 142432, Russia*

²*Institute of Problems of Chemical Physics, Russian Academy of Sciences, Chernogolovka, Moscow Region 142432, Russia*

³*Lomonosov Moscow State University, Moscow 119991, Russia*

⁴*National University of Science and Technology "MISIS," Moscow 119049, Russia*

⁵*National Research South Ural State University, Chelyabinsk 454080, Russia*

⁶*Ural Federal University, 620002 Ekaterinburg, Russia*



(Received 5 November 2019; revised manuscript received 6 March 2020; accepted 25 March 2020; published 23 April 2020)

Fluorine NMR is performed on two ReF_6 -based single-molecule magnets, a conductor, $(\text{BEDO})_4[\text{ReF}_6] \cdot 6\text{H}_2\text{O}$, and its parent substance, an insulator, $(\text{PPh}_4)_2[\text{ReF}_6] \cdot 2\text{H}_2\text{O}$. The correlation frequency of electronic spin fluctuations, ω_c , is derived from the spin-lattice relaxation rate. These data, combined with the inverse decay time of the magnetization, $1/\tau_c$, determined from the low-frequency ac susceptibility measurements, allows tracking of the spin dynamics span over seven orders of magnitude. We demonstrate that the two data sets, $1/\tau_c$ and the low-temperature region of ω_c , can be described by the same model, which includes Orbach, Raman, and “quantum tunneling of magnetization” contributions. This indicates that the two techniques characterize the same process. The influence of the conduction electrons on spin-lattice relaxation in $(\text{BEDO})_4[\text{ReF}_6] \cdot 6\text{H}_2\text{O}$ is revealed below 25 K as a trend of the relaxation to follow a linear temperature dependence.

DOI: [10.1103/PhysRevB.101.134427](https://doi.org/10.1103/PhysRevB.101.134427)

I. INTRODUCTION

The phenomenon of molecular magnetism, discovered in the early 1990s [1–5], has aroused wide interest in the physical community. The so-called single-molecule magnet (SMM) is a metal complex in which paramagnetic centers, usually high-spin ions or ion clusters of individual molecules, are isolated from each other by bulky ligands. Magnetic interactions between neighboring molecules of such a system are negligible, thus its bulk magnetic properties are determined mainly by intramolecular interactions, allowing us to consider them ensembles of separate nanoscopic-sized magnets. Owing to their specific properties such as slow relaxation of magnetization, blocking, and quantum tunneling of magnetization (QTM) [6–9], SMMs have been regarded as very attractive objects for both academic studies and applications in promising areas of technology and electronics like quantum computing [10,11], memory cells [5], and spintronics [9,12].

Recently, the interest in molecular magnetism has shifted to engineering of and research on polyfunctional materials that combine various useful properties or functions, such as SMM and conductivity, within a single structural unit [13]. However, the first attempts to synthesize conductive materials with SMM properties resulted in semiconductor-type systems, possessing a reasonably high electrical conductivity at high temperatures but demonstrating the transport properties of an insulator at low temperatures where the SMM-specific features just start to be manifested. The recently synthesized

complex $(\text{BEDO})_4[\text{ReF}_6] \cdot 6\text{H}_2\text{O}$ [14] (BEDO- ReF_6) studied in this report is, among quite a few systems, the single one, to our knowledge, in which the reasonably high conductivity provided by BEDO radical cations and single-molecule magnetism due to $[\text{ReF}_6]^{2+}$ anions [15] coexist in the same temperature range.

Undoubtedly, studying the quantum properties of SMMs at ultralow temperatures is of the greatest research interest. On the other hand, understanding the mechanisms of relaxation and decoherence in SMMs is important for fundamental knowledge and valuable for practical manipulations of the electronic spin properties of molecular nanomagnets. Therefore, information on spin dynamics over the entire temperature range, from uncorrelated spins at high temperatures to their collective state at low temperatures, is also significant.

Nuclear magnetic resonance (NMR) studies of various SMMs [16] have pointed to a universal nuclear spin-lattice relaxation mechanism related to a characteristic frequency ω_c in the excitation spectrum of electronic spin fluctuations. Early on it was realized [17–21] that in fact ω_c , or the decay time $\tau_c = 1/\omega_c$, characterizes the relaxation process of the total magnetization of the SMM, M , driven by spin-phonon interaction. The strongly temperature-dependent ω_c decreases dramatically, by several decades, upon cooling from moderately high temperatures (ca. 100 K) down to the low-temperature QTM region (usually below 4.2 K) [19]. When ω_c lies in the region of Larmor frequencies of NMR it can be probed with nuclear spin-lattice relaxation rate measurements. At lower temperatures, ω_c falls down to the acoustic frequency range and can be accessed by conventional ac susceptibility techniques.

*vyasel@issp.ac.ru

In this paper we report ^{19}F NMR experiments performed on BEDO-ReF6 and its parent complex $(\text{PPh}_4)_2[\text{ReF}_6] \cdot 2\text{H}_2\text{O}$ (PPh4-ReF6). The temperature dependences of ω_c extracted from the measured spin-lattice relaxation rate are presented and described together with the low-temperature/low-frequency data obtained from the ac susceptibility published previously [14,15].

II. EXPERIMENTAL PROCEDURE

The measurements on BEDO-ReF6 reported in this paper were done on the same powder sample, $m = 9.56$ mg, used for ac susceptibility measurements in a recent publication [14], where the details of its synthesis and structure are also presented. The dc susceptibility, χ , required to analyze the NMR data was measured under an applied field of 1 kG in a field-cooled regime using the VMS option of a Quantum Design PPMS-9T magnetometer.

An ~ 10 -mg powder sample of PPh-ReF6 was used for NMR. NMR was measured under an applied field of 7 T using a Bruker MSL300 spectrometer equipped with an Oxford CF1200 flow cryostat.

The fluorine spin-lattice relaxation was measured using standard saturation-recovery pulse sequence, $10 \times (t_{\pi/2} - t') - \tau - t_{\pi/2} - \tau' - t_{\pi} - \tau'$, acquisition, with $\pi/2$ pulse length $t_{\pi/2} = 1 \mu\text{s}$ and $\tau' = 10 \mu\text{s}$. The measured saturation-recovery transients $M(\tau)$ were not simple single-exponential functions, which often happens in systems in which nuclear spins relax in different environments of magnetic ions and thus have different relaxation rates [22,23]. In this case the spin-lattice relaxation time, T_1 , can be evaluated using a stretched-exponential function,

$$M(\tau) = M_{\infty}(1 - \exp(-\tau/T_1)^p), \quad (1)$$

with $0.5 \leq p \leq 1$. For both samples, expression (1) provided excellent fits to the measured saturation-recovery transients over the whole temperature range. In order to illustrate this we plot in Fig. 1 the value $\ln[1 - M(\tau)/M_{\infty}]$ as a function of $(\tau/T_1)^p$, where T_1 and p are parameters derived from the fits with Eq. (1) to $M(\tau)$ measured in BEDO-ReF6 at $T = 4.2$, 50, and 271 K. One can see that, as expected, in this presentation the recovery curve at either temperature is a straight line with a slope of -1 . Temperature dependences of the derived parameter p are presented in Fig. S2 of the Supplemental Material [24].

The samples are apparently stable over many months. First, NMR data on BEDO-ReF6 were taken immediately upon completion of the susceptibility measurements. Eighteen months later when all NMR data had been collected, we remeasured the NMR at several temperatures in the range 5–200 K and found no change either in the spectrum shape or in the relaxation times, T_1 and T_2 .

III. RESULTS AND DISCUSSION

Temperature dependences of the product $\chi_{\text{Re}}T$ and of $1/\chi_{\text{Re}}$ for BEDO-ReF6 are presented in Fig. 2. Here χ_{Re} is the T -dependent contribution to the total measured susceptibility, χ , related to $5d$ Re^{4+} moments: $\chi_{\text{Re}} = \chi - \chi_0$. The T -independent term $\chi_0 \cong 0.005$ emu/mol is the sum of the

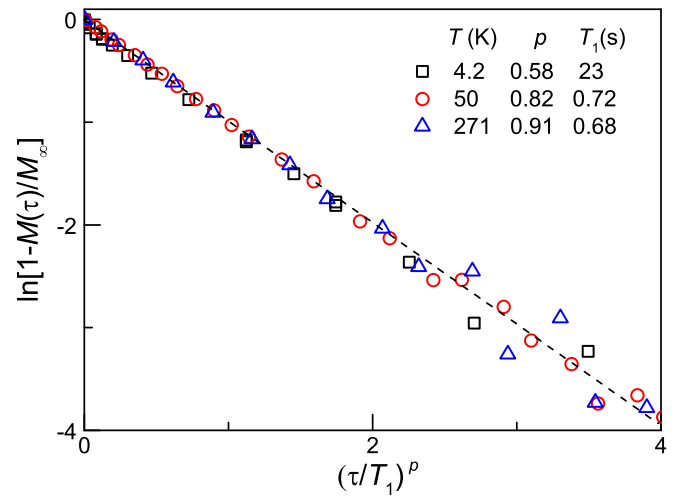


FIG. 1. ^{19}F spin-lattice relaxation curves for BEDO-ReF6 at $T = 4.2$ K (squares), $T = 50$ K (circles), and $T = 271$ K (triangles) as a function of the reduced delay $(\tau/T_1)^p$. Parameters T_1 and p are derived from the fits with Eq. (1) to the measured $M(\tau)$.

diamagnetic contribution from the closed electronic shells and the paramagnetic one related to conduction electrons.

The apparent linearity of $1/\chi_{\text{Re}}(T)$ in Fig. 2 suggests the Curie law $\chi_{\text{Re}} = C/T$ with $C = 1.3$ emu $\cdot (\text{mol} \cdot \text{K})^{-1}$, corresponding to $\mu_{\text{eff}} = 3.22\mu_B$. However, the $\chi_{\text{Re}}T$ product reveals a decrease below this value at low temperatures. The origin of this decrease should be the same as in the precursor compound PPh-ReF6, where it has also been observed and ascribed to single-ion anisotropy (zero-field splitting) [15], because large distances between $[\text{ReF}_6]^{2+}$ ions makes interaction between them unlikely.

The ^{19}F NMR peak in PPh-ReF6 is about twice as broad as in BEDO-ReF6 (see Fig. S1 of the Supplemental Material [24]) over the whole temperature range. Upon cooling, its full width at half-maximum increases from 25 kHz at 273 K to 250 kHz at 15 K. The spin-spin relaxation time, T_2 , in both

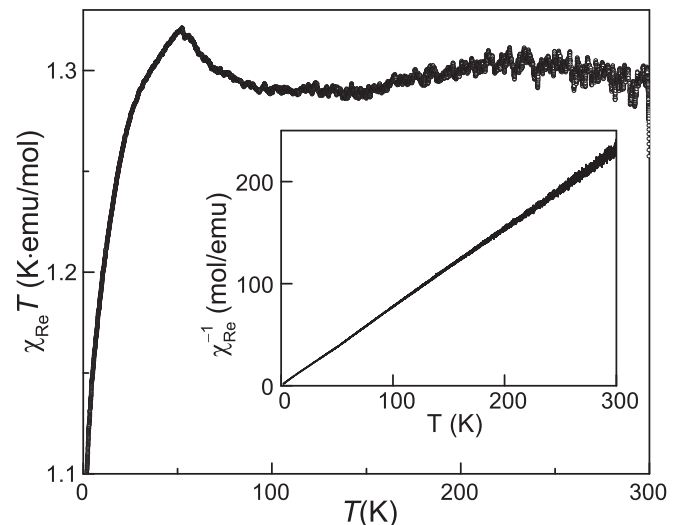


FIG. 2. Temperature dependence of the $\chi_{\text{Re}}T$ product for BEDO-ReF6. Inset: Temperature dependence of $1/\chi_{\text{Re}}$.

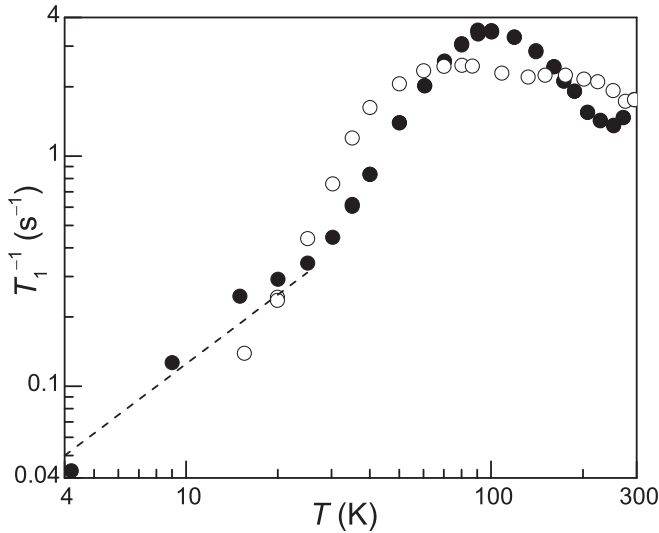


FIG. 3. Temperature dependences of the fluorine spin-lattice relaxation rates in PPh-ReF6 (open circles) and BEDO-ReF6 (filled circles). The dashed line represents $T_1^{-1} \propto T$.

samples decreases from 150 to 25 μs in the same temperature interval. The extreme growth of the linewidth and spin-spin relaxation rate, T_2^{-1} , known as the “wipeout effect” [25], results in a dramatic decrease in the signal intensity at low temperatures. In combination with the quite long T_1 , this makes data acquisition rather problematic. That is why the data for PPh-ReF6 below 15 K could not be collected with a reasonable signal-to-noise ratio.

The fluorine spin-lattice relaxation rates, T_1^{-1} , measured in PPh-ReF6 and BEDO-ReF6 are shown as a function of the temperature in Fig. 3. As in many other SMMs such as molecular rings and clusters with $3d$ metals [16,22,26], the relaxation rate of both of the studied compounds is nonmonotonous in temperature and demonstrates a prominent peak around a temperature $T_p = 95 \pm 5$ K for BEDO-ReF6 and $T_p = 75 \pm 5$ K for PPh-ReF6. Upon cooling below T_p , T_1^{-1} in both compounds decreases rapidly; however, in BEDO-ReF6 the T dependence of the relaxation rate below $T \sim 30$ K is less steep, close to the $T_1^{-1} \propto T$ behavior shown by the dashed line in Fig. 3.

The spin of the fluorine nucleus is $1/2$, which means that its spin-lattice relaxation can only be caused by ^{19}F Larmor-frequency fluctuations of an effective magnetic field induced at the nucleus site. In PPh-ReF6 and BEDO-ReF6 the relevant field is the hyperfine field from the local magnetic moments of Re^{4+} . The case is very similar to the proton relaxation in $3d$ -metal-based molecular rings [16,22,27] so the approach developed for its analysis can be utilized for T_1^{-1} data in ReF_6 -based systems. The approach is based on Moriya’s theory of nuclear relaxation in paramagnets [28]. Assuming that both the relaxation and the fluctuation of Re ion magnetization are driven by a dominant single correlation frequency, ω_c , that modulates the hyperfine field at the nuclear site [27,29], the expression for the relaxation rate is

$$T_1^{-1} = A\chi_{\text{Re}}T \frac{\omega_c(T)}{\omega_c^2(T) + \omega_L^2}, \quad (2)$$

where ω_L is the fluorine Larmor frequency and A expresses the square hyperfine (dipolar) coupling. In order to extract $\omega_c(T)$ from the measured T_1^{-1} data, we construct the normalized relaxation rate,

$$R = \frac{1}{T_1\chi_{\text{Re}}T} = A \frac{\omega_c(T)}{\omega_c^2(T) + \omega_L^2}. \quad (3)$$

For BEDO-ReF6 we use the $\chi_{\text{Re}}T$ shown in Fig. 2; the data for PPh-ReF6 have been taken from Ref. [15]. Strictly speaking, χ_{Re} measured at the same field as T_1 , that is, 7 T, should have been used here. However, we believe that we can safely use the low-field (0.1 T) data for χ_{Re} because we stay in the low-field, high-temperature regime $\mu_B H \ll k_B T$ ($T > 25$ K for BEDO-ReF6, $T > 15$ K for PPh-ReF6). In this temperature range χ_{Re} values in both samples demonstrate temperature dependences of a Curie-type paramagnet, C/T , and also a linear field magnetization (see Fig. 2 for BEDO-ReF6 and Fig. 2 in Ref. [15]), which implies a field-independent susceptibility.

The temperature dependences of R (shown in Fig. S3 of the Supplemental Material [24]) are qualitatively the same as $T_1^{-1}(T)$ (Fig. 3) because of the gradual behavior of $\chi T(T)$ in both samples, with the maxima in $R(T)$ appearing at the same temperature, T_p , as in $T_1^{-1}(T)$. According to Eq. (3), the maximum value of $R_p = R(T_p)$ is reached when $\omega_c(T) = \omega_L$, which yields $R_p = A/2\omega_L = 2.7$ and 1.75 ($\text{s} \cdot \text{K} \cdot \text{emu/mol}$) $^{-1}$ for BEDO-ReF6 and PPh-ReF6, respectively. Finally, we make the substitution $A = 2R_p\omega_L$ in Eq. (3) and solve it with respect to ω_c .

The resulting temperature dependences of ω_c for BEDO-ReF6 and PPh-ReF6 derived from the nuclear spin-lattice relaxation data are shown in Fig. 4. For BEDO-ReF6 we have omitted the data below $T \sim 25$ K where the relaxation through conduction electrons becomes significant, according to Fig. 3.

As shown in Fig. 4, ω_c at $T < T_p$ follows a power-law T dependence $\omega_c \propto T^n$ with $n \sim 2.3 \pm 0.1$, similarly to $3d$ -metal-based SMM complexes, where $\omega_c \propto T^{3.5 \pm 0.5}$ [22]. The normalized relaxation rate, $R(T)$, calculated using Eq. (3) with $\omega_c \propto T^n$, is plotted in Fig. S3 of the Supplemental Material [24].

In the same plot with ω_c data derived from NMR (Fig. 4), we show the values $\omega_c = 1/\tau_c$ obtained from the low-frequency (≤ 10 -kHz) measurements of the imaginary part of the dynamic susceptibility, χ'' , reported in Refs. [14,15]. As one can see, the two data sets span over 10^7 of the change in ω_c , going from 2 to 300 K. Though we are currently lacking the data in the region 4–15 K (up to 25 K for BEDO-ReF6), we attempted to fit the ω_c data obtained from both NMR and low-frequency ac susceptibility measurements, χ'' , with the sum of the Orbach, Raman, and T -independent QTM contributions [30],

$$\omega_c = \tau_{\text{Orb}}^{-1} + \tau_{\text{Ram}}^{-1} + \tau_{\text{QTM}}^{-1}, \quad (4a)$$

where

$$\tau_{\text{Orb}} = \tau_0 \exp(\Delta/k_B T), \quad (4b)$$

$$\tau_{\text{Ram}} = C_{\text{Ram}} T^{-m}, \quad (4c)$$

$$\tau_{\text{QTM}} = \text{const.} \quad (4d)$$

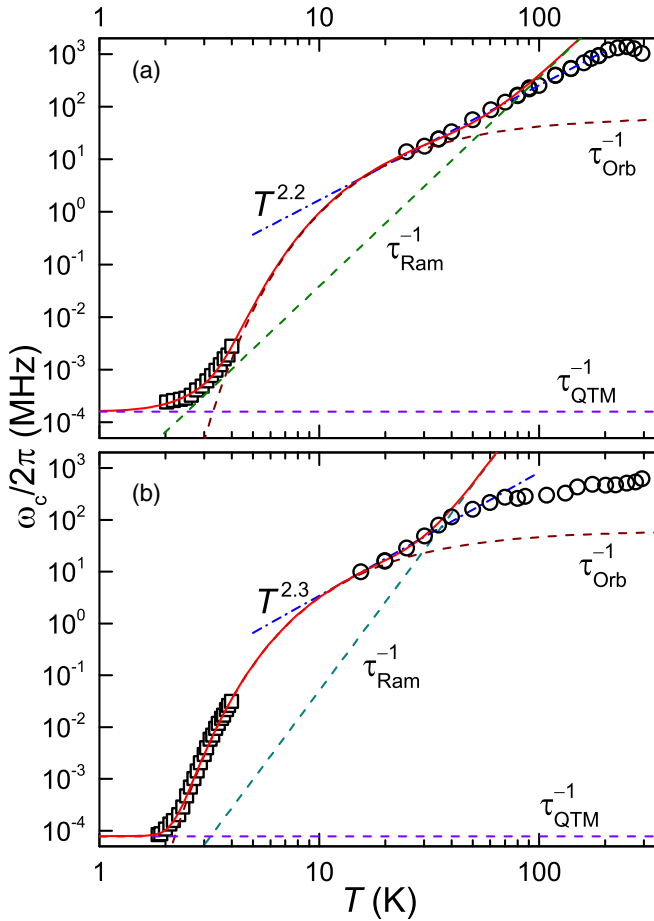


FIG. 4. Temperature dependences of the correlation frequency of electronic spin fluctuations, ω_c , extracted from the fluorine spin-lattice relaxation rate (circles), and the inverse decay time of the magnetization, $1/\tau_c$, determined from the low-frequency ac susceptibility measurements (squares) for (a) BEDO-ReF6 and (b) PPh-ReF6. Dash-dotted blue lines are power-law fits to the data at a moderately high temperature. Solid red lines are best fits to low- T data using Eqs. (4).

Quite expectedly, Eqs. (4) fail to describe the whole range of $\omega_c(T)$ data in Fig. 4. Prioritizing to best fit the low-temperature/low-frequency region of ω_c obtained directly from the ac susceptibility measurements, we successively lowered the upper T -range limit of the $\omega_c(T)$ NMR data set until the extracted fit parameters changed negligibly upon subsequent iteration. The fits converged for BEDO-ReF6 at $T \leq 90$ K and for PPh-ReF6 at $T \leq 40$ K, as shown in Fig. 4, with parameters listed in Table I.

In Fig. 5 we plot the inverse values, $1/\omega_c = \tau_c$, as a function of $1/T$, together with the fits according to Eqs. (4) with parameters listed in Table I, to illustrate the quality of the fits to the low-frequency/low-temperature data.

The normalized relaxation rate, $R(T)$, calculated using Eq. (3) with ω_c in the form of Eq. (4) with parameters listed in Table I, is plotted in Fig. S3 of the Supplemental Material [24].

As one can see in Figs. 4 and 5, Eqs. (4) provide adequate fits to the low-temperature data obtained from the ac χ measurements and track at least five orders of magnitude of

TABLE I. Components of Eq. (4a) with parameters obtained from the fits to ω_c (Fig. 4) in the range 2–40 K for Ph4P-ReF6 and 2–90 K for BEDO-ReF6. All τ 's are given in seconds; T should be taken in kelvins.

	Ph4P-ReF6	BEDO-ReF6
τ_{Orb}	$2.5 \times 10^{-9} \exp(30/T)$	$2.5 \times 10^{-9} \exp(42/T)$
τ_{Ram}	$1.5T^{-5.7}$	$0.04T^{-4}$
τ_{QTM}	2×10^{-3}	10^{-3}

the temperature growth of ω_c up to the NMR range. This description is more thorough compared to the single-component Orbach-type fits suggested in Refs. [14, 15]. According to the parameters extracted from the fits, both studied systems exhibit similar magnetization dynamics, especially concerning Orbach and QTM contributions. A rather big difference in the Raman contributions to ω_c originate, probably, in the crystal structure: the apical distances in BEDO-ReF6 are essentially shortened [14] compared to those in PPh-ReF6. What is most important, Eqs. (4) enable a bridge between ω_c data derived from ac χ and from NMR, indicating that the two experimental techniques indeed probe the same physical quantity. This

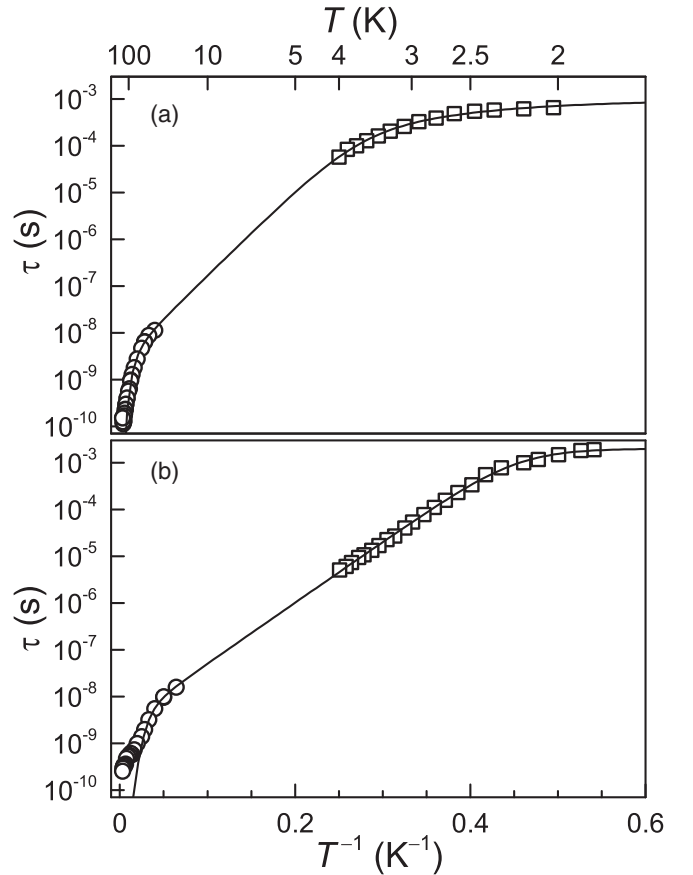


FIG. 5. Decay time $\tau_c = 1/\omega_c$ (reciprocals of the data shown in Fig. 4) as a function of the inverse temperature for (a) BEDO-ReF6 and (b) PPh-ReF6. Circles, NMR; squares, ac χ . Solid lines represent the inverse of Eq. (4a) with parameters listed in Table I.

clearly demonstrates the possibility of measuring ω_c using different experimental methods, as suggested before [18].

IV. SUMMARY

Fluorine NMR of two $[\text{ReF}_6]^{-2}$ -ion-based SMMs, one insulating (PPh-ReF6) and the other conducting (BEDO-ReF6), has been performed. Analysis of the spin-lattice relaxation has yielded temperature dependences of the characteristic frequency of electronic spin fluctuations, ω_c . In combination with the inverse decay time of the magnetization, $1/\tau_c$, determined from the low-frequency ac susceptibility measurements, it enables tracking of the spin dynamics in studied SMMs over seven orders of magnitude. A model that includes Orbach, Raman, and QTM contributions to the magnetization relaxation bridges the data obtained by the two rather different experimental techniques, which infers that they indeed probe the same physical quantity. In terms of magnetic properties the two studied systems are found to be essentially alike.

However, in the conductor BEDO-ReF6 the nuclear spin-lattice relaxation at $T < 30$ K tends to T -linear dependence, which implies that conduction-electron-mediated relaxation becomes the dominant relaxation mechanism.

ACKNOWLEDGMENTS

The authors are grateful to A. V. Palii for useful discussions and suggestions. This work was supported by RFBR Grant No. 17-03-00167. One of the authors (N.D.K.) received support also from RFBR Grant No. 18-02-00280. This work was partially supported by the Ministry of Education and Science of the Russian Federation in the framework of Increase Competitiveness Program of NUST “MISiS” Grant No. K2-2020-008; by Act 211 of the Government of Russian Federation, Contract Nos. 02.A03.21.0004, 02.A03.21.0006, and 02.A03.21.0011; and by State task No. AAAA-A19-111902390079-8 for the IPCP RAS.

-
- [1] A. Caneschi, D. Gatteschi, R. Sessoli, A. L. Barra, L. C. Brunel, and M. Guillot, *J. Am. Chem. Soc.* **113**, 5873 (1991).
- [2] R. Sessoli, H. L. Tsai, A. R. Schake, S. Wang, J. B. Vincent, K. Folting, D. Gatteschi, G. Christou, and D. N. Hendrickson, *J. Am. Chem. Soc.* **115**, 1804 (1993).
- [3] R. Sessoli, D. Gatteschi, A. Caneschi, and M. A. Novak, *Nature* **365**, 141 (1993).
- [4] S. M. J. Aubin, M. W. Wemple, D. M. Adams, H.-L. Tsai, G. Christou, and D. N. Hendrickson, *J. Am. Chem. Soc.* **118**, 7746 (1996).
- [5] G. Christou, D. Gatteschi, D. N. Hendrickson, and R. Sessoli, *MRS Bull.* **25**, 66 (2000).
- [6] J. R. Friedman, M. P. Sarachik, J. Tejada, J. Maciejewski, and R. Ziolo, *J. Appl. Phys.* **79**, 6031 (1996).
- [7] L. Thomas, F. Lioni, R. Ballou, D. Gatteschi, R. Sessoli, and B. Barbara, *Nature* **383**, 145 (1996).
- [8] S. J. Blundell, in *Magnetism: A Synchrotron Radiation Approach*, edited by E. Beaurepaire, H. Bulou, F. Scheurer, and J.-P. Kappler (Springer, Berlin, 2006), pp. 345–373.
- [9] J. Bartolomé, F. Luis, and J. F. Fernández (eds.), *Molecular Magnets: Physics and Applications* (Springer, Berlin, 2014).
- [10] M. N. Leuenberger and D. Loss, *Nature* **410**, 789 (2001).
- [11] J. Tejada, E. M. Chudnovsky, E. del Barco, J. M. Hernandez, and T. P. Spiller, *Nanotechnology* **12**, 181 (2001).
- [12] L. Bogani and W. Wernsdorfer, *Nanoscience and Technology*, edited by P. Rodgers (World Scientific, Singapore, 2009), pp. 194–201.
- [13] G. Cosquer, Y. Shen, M. Almeida, and M. Yamashita, *Dalton Trans.* **47**, 7616 (2018).
- [14] N. D. Kushch, L. I. Buravov, P. P. Kushch, G. V. Shilov, H. Yamochi, M. Ishikawa, A. Otsuka, A. A. Shakin, O. V. Maximova, O. S. Volkova, A. N. Vasiliev, and E. B. Yagubskii, *Inorg. Chem.* **57**, 2386 (2018).
- [15] K. S. Pedersen, M. Sigrist, M. A. Sørensen, A.-L. Barra, T. Weyhermüller, S. Piligkos, C. A. Thuesen, M. G. Vinum, H. Mutka, H. Weihe, R. Clérac, and J. Bendix, *Angew. Chem. Int. Ed.* **53**, 1351 (2014).
- [16] S. H. Baek, M. Luban, A. Lascialfari, E. Micotti, Y. Furukawa, F. Borsa, J. van Slageren, and A. Cornia, *Phys. Rev. B* **70**, 134434 (2004).
- [17] P. Santini, S. Carretta, E. Livioti, G. Amoretti, P. Carretta, M. Filibian, A. Lascialfari, and E. Micotti, *Phys. Rev. Lett.* **94**, 077203 (2005).
- [18] I. Rousochatzakis, *Phys. Rev. B* **76**, 214431 (2007).
- [19] I. Rousochatzakis, A. Läuchli, F. Borsa, and M. Luban, *Phys. Rev. B* **79**, 064421 (2009).
- [20] A. Keren, O. Shafir, E. Shimshoni, V. Marvaud, A. Bachschmidt, and J. Long, *Phys. Rev. Lett.* **98**, 257204 (2007).
- [21] Z. Salman, A. Keren, P. Mendels, V. Marvaud, A. Sculler, M. Verdagner, J. S. Lord, and C. Baines, *Phys. Rev. B* **65**, 132403 (2002).
- [22] F. Borsa, in *NMR-MRI, μ SR and Mössbauer Spectroscopies in Molecular Magnets*, edited by P. Carretta and A. Lascialfari (Springer, Milan, 2007), pp. 29–70.
- [23] G. B. Furman, A. M. Panich, A. Yochelis, E. M. Kunoff, and S. D. Goren, *Phys. Rev. B* **55**, 439 (1997).
- [24] See Supplemental Material at <http://link.aps.org/supplemental/10.1103/PhysRevB.101.134427> for the NMR spectra of fluorine, the temperature dependence of parameter p in Eq. (1), and the temperature dependences of the reduced spin-lattice relaxation rate, Eq. (3).
- [25] M. Belesi, A. Lascialfari, D. Prociassi, Z. H. Jang, and F. Borsa, *Phys. Rev. B* **72**, 014440 (2005).
- [26] H. Amiri, A. Lascialfari, Y. Furukawa, F. Borsa, G. A. Timco, and R. E. P. Winpenny, *Phys. Rev. B* **82**, 144421 (2010).
- [27] H. Amiri, M. Mariani, A. Lascialfari, F. Borsa, G. A. Timco, F. Tuna, and R. E. P. Winpenny, *Phys. Rev. B* **81**, 104408 (2010).
- [28] T. Moriya, *Prog. Theor. Phys.* **16**, 23 (1956).
- [29] C. P. Slichter, *Principles of Magnetic Resonance* (Springer, Berlin, 1990).
- [30] F.-S. Guo, B. M. Day, Y.-C. Chen, M.-L. Tong, A. Mansikkamäki, and R. A. Layfield, *Science* **362**, 1400 (2018).